Review Article
Bulletin of Pure and Applied Sciences.
Chemistry , Vol.44 C, No.2
July-December 2025: P. 144-154

http://www.bpasjournals.com/chemistry
Print version ISSN 0970 4620
Online version ISSN 2320 320X

Decoding Aluminum Distribution in SSZ-13 Zeolites: Effects of Synthesis Parameters and Post-Treatment Protocols

[1]Chinaza F. Nwachukwu, [2]Ann Mati

Author's Affiliations:
[1]Tulane University, New Orlean, Louisiana
[2]Texas Tech University, Department of Chemical Engineering, Lubbock, Texas
chinazanwagod@gmail.com

ABSTRACT

SSZ-13 zeolites with chabazite (CHA) topology are pivotal in industrial catalysis, particularly in methanol-to-olefins (MTO) conversion and selective catalytic reduction (SCR) of nitrogen oxides. The catalytic efficiency of these materials is governed by the spatial distribution of aluminum (Al) atoms within the silica framework, which dictates the nature and availability of active sites. This study investigates the impact of synthesis parameters and post-synthesis treatments on Al distribution in SSZ-13 zeolites, with a focus on paired versus isolated Al sites. By systematically varying the ratios of organic ($TMAda^+$) and inorganic (Na^+) structure-directing agents during synthesis, the critical role of these agents in modulating Al arrangements is demonstrated. Low $Na^+/TMAda^+$ ratios favored isolated Al sites, enhancing Brønsted acidity, whereas intermediate ratios promoted Al pairing, facilitating divalent cation stabilization, such as Co^{2+}. Beyond a threshold ratio, phase transitions to mordenite (MOR) were observed, underscoring the delicate balance required for CHA formation. Post-synthesis treatments, including alternative drying protocols, further influenced Al distribution, with deviations from standardized methods predominantly yielding isolated Al sites and reducing Co^{2+} ion-exchange capacity. Cation-exchange experiments and spectroscopic analyses provided quantitative insights into Al arrangements, highlighting a strong correlation between synthesis conditions, framework stability, and catalytic performance. The findings emphasize the need for precise control of synthesis and post-treatment protocols to tailor SSZ-13 properties for specific applications. This work offers a framework for optimizing SSZ-13 zeolites by linking Al distribution to catalytic functionality, paving the way for advancements in industrial catalysis and the rational design of zeolitic materials. Future research should explore standardized post-synthesis treatments and expand topological studies to enhance reproducibility and generalizability

Keywords: SSZ-13 zeolite, aluminum distribution, structure-directing agents, chabazite, methanol-to-olefins, selective catalytic reduction

How to cite this article: Chinaza F. Nwachukwu, Ann Mati. Decoding Aluminum Distribution in SSZ-13 Zeolites: Effects of Synthesis Parameters and Post-Treatment Protocols. *Bulletin of Pure and Applied Sciences-Chemistry,* 2025;44C (2):144-154.

1. INTRODUCTION

Zeolites represent a class of crystalline aluminosilicate materials characterized by their well-defined microporous structures, high surface areas, and tunable acidity (Dědeček et al., 2012; Deimund et al., 2016; Gallego et al., 2018). These properties render zeolites indispensable in numerous industrial applications, including catalysis, adsorption, and ion exchange. Among the diverse zeolite frameworks, SSZ-13 with chabazite (CHA) topology has emerged as particularly significant due to its exceptional performance in methanol-to-olefins (MTO) conversion and selective catalytic reduction (SCR) of nitrogen oxides (NOx) (Zhu et al., 2008; Nishitoba et al., 2018; Khivantsev et al., 2024). The catalytic behavior of SSZ-13 zeolites is intrinsically linked to the spatial arrangement of aluminum (Al) atoms within the silica framework. Framework Al atoms generate Brønsted acid sites that serve as active centers for catalytic transformations (Dědeček et al., 2012; Di Iorio & Gounder, 2016). The distribution of these Al atoms, whether isolated or paired, profoundly influences the strength and accessibility of acid sites, as well as the ability to stabilize extra-framework cations such as Cu^{2+} and Co^{2+} (Bates et al., 2014; Paolucci et al., 2016; Mlekodaj et al., 2019). Paired Al sites, characterized by two Al atoms in close proximity within the zeolite framework, can accommodate divalent cations, thereby enhancing ion-exchange capacity and catalytic versatility (Gao et al., 2013; Di Iorio et al., 2017). Despite the recognized importance of Al distribution, achieving precise control over Al placement during zeolite synthesis remains a formidable challenge. The synthesis of SSZ-13 typically involves the use of structure-directing agents (SDAs), which template the formation of specific framework topologies (Wang et al., 2022). Organic SDAs, such as N,N,N-trimethyl-1-adamantylammonium ($TMAda^+$), and inorganic SDAs, such as sodium ions (Na^+), play complementary roles in directing framework assembly and influencing Al distribution (Di Iorio et al., 2020). The interplay between these SDAs during crystallization governs not only the framework topology but also the arrangement of Al atoms within the structure (Devos et al., 2020).
Post-synthesis treatments, including calcination, ion exchange, and drying protocols, further modulate the Al distribution and framework stability of SSZ-13 zeolites (Nishitoba et al., 2018). Variations in these treatments can lead to significant differences in catalytic performance, even for zeolites synthesized under nominally identical conditions. Understanding the effects of post-synthesis protocols is therefore essential for ensuring reproducibility and optimizing zeolite properties for target applications. This study investigates the influence of synthesis parameters, particularly the $Na^+/TMAda^+$ ratio, and post-synthesis treatments on Al distribution in SSZ-13 zeolites. By employing cobalt ion-exchange experiments as a quantitative probe for paired Al sites, coupled with spectroscopic characterization, the relationships between synthesis conditions, Al arrangements, and catalytic properties are elucidated. The findings provide insights into strategies for tailoring SSZ-13 zeolites with controlled Al distributions, thereby advancing the rational design of zeolitic materials for industrial catalysis.

2. LITERATURE REVIEW

2.1 Aluminum Distribution and Catalytic Performance

The catalytic activity of zeolites is fundamentally determined by the nature and distribution of framework Al atoms, which generate Brønsted acid sites upon protonation (Deimund et al., 2016). In SSZ-13 zeolites, isolated Al sites contribute to stronger Brønsted acidity, making them particularly effective for reactions requiring high acid strength, such as alkane cracking and isomerization (Gallego et al., 2018). Conversely, paired Al sites, where two Al atoms reside in close proximity within the framework, facilitate the stabilization of divalent cations, which are crucial for redox catalysis in SCR applications (Mlekodaj et al., 2019; Khivantsev et al., 2024). The spatial arrangement of Al atoms also affects the hydrothermal stability of zeolites. Studies have shown that zeolites with predominantly isolated Al sites exhibit enhanced resistance to dealumination under harsh hydrothermal conditions, thereby maintaining their structural integrity and catalytic activity over extended periods (Nishitoba et al., 2018). In contrast, zeolites with higher fractions of paired Al sites may experience framework degradation more readily, although the presence of stabilizing cations can mitigate this effect (Di Iorio et al., 2020). Recent advances in spectroscopic techniques, including solid-state nuclear magnetic resonance (NMR) and X-ray absorption spectroscopy (XAS), have enabled more detailed characterization of Al distributions in zeolites (Mlekodaj et al., 2019). These techniques, combined with computational modeling, have provided mechanistic insights into how Al arrangements

influence catalytic pathways and selectivity (Wang et al., 2022).

2.2 Role of Structure-Directing Agents in Zeolite Synthesis

Structure-directing agents (SDAs) are organic or inorganic molecules that template the formation of specific zeolite frameworks during hydrothermal synthesis (Di Iorio & Gounder, 2016). Organic SDAs, such as $TMAda^+$, occupy the pore spaces of the developing zeolite structure, guiding the assembly of silicate and aluminate species into the desired topology (Devos et al., 2020). The bulky, rigid structure of $TMAda^+$ makes it particularly effective for directing the formation of small-pore zeolites like SSZ-13 with CHA topology. Inorganic SDAs, such as alkali metal cations (e.g., Na^+, K^+), also play critical roles in zeolite synthesis by balancing framework charges and influencing crystallization kinetics (Di Iorio et al., 2020). The choice and concentration of inorganic SDAs can significantly affect the Al distribution within the zeolite framework. For instance, higher Na^+ concentrations have been shown to promote Al pairing by facilitating the incorporation of multiple Al atoms in close proximity, whereas lower Na^+ concentrations favor isolated Al sites (Nishitoba et al., 2018). The synergistic effects of organic and inorganic SDAs have been exploited to achieve fine control over Al distributions in SSZ-13 zeolites (Di Iorio et al., 2020). By systematically varying the $Na^+/TMAda^+$ ratio, researchers have demonstrated the ability to tune the fraction of paired versus isolated Al sites, thereby tailoring the zeolite properties for specific catalytic applications (Wang et al., 2022). However, excessive SDA concentrations can lead to undesired phase transitions, such as the formation of mordenite (MOR) instead of CHA, highlighting the importance of optimizing synthesis conditions (Di Iorio & Gounder, 2016).

2.3 Quantification of Paired Aluminum Sites

Quantifying the distribution of Al atoms in zeolites, particularly the fraction of paired versus isolated sites, is essential for understanding structure-activity relationships (Mlekodaj et al., 2019). One widely used approach involves cation-exchange experiments with divalent cations such as Co^{2+} or Cu^{2+}, which preferentially occupy paired Al sites due to the requirement for two charge-compensating framework oxygens (Di Iorio et al., 2017). The saturation capacity of Co^{2+} exchange, determined from ion-exchange isotherms, provides a quantitative measure of the fraction of paired Al sites in the zeolite (Mlekodaj et al., 2019). Spectroscopic techniques complement cation-exchange studies by providing direct structural information about Al environments. For example, ^{27}Al magic-angle spinning (MAS) NMR spectroscopy can distinguish between tetrahedral and octahedral Al coordination, as well as provide insights into the local environment of framework Al atoms (Devos et al., 2020). Infrared (IR) spectroscopy, particularly using probe molecules such as pyridine or CO, can characterize the strength and accessibility of Brønsted acid sites associated with framework Al (Nishitoba et al., 2018). Advanced characterization methods, including extended X-ray absorption fine structure (EXAFS) and diffuse reflectance UV-Vis spectroscopy, have been employed to probe the coordination and oxidation states of exchanged cations, providing further insights into Al distributions (Mlekodaj et al., 2019; Khivantsev et al., 2024). Computational studies using density functional theory (DFT) have also contributed to understanding the thermodynamic and kinetic factors governing Al placement during zeolite synthesis (Wang et al., 2022).

2.4 Post-Synthesis Treatments and Framework Stability

Post-synthesis treatments, including calcination, ion exchange, and drying, are critical steps in zeolite preparation that can significantly influence Al distribution and framework stability (Nishitoba et al., 2018). Calcination, typically performed at temperatures between 500-600°C, removes the organic SDA from the zeolite pores, generating Brønsted acid sites. However, the calcination conditions (temperature, atmosphere, heating rate) can affect the extent of dealumination and the distribution of extra-framework Al species (Devos et al., 2020). Drying protocols, particularly those involving controlled atmosphere and temperature, are essential for preserving the integrity of the zeolite framework and maintaining the desired Al distribution (Di Iorio et al., 2020). Deviations from standardized drying procedures, such as variations in air flow or humidity, can lead to framework distortions and alterations in Al arrangements, as observed in studies comparing zeolites dried using Indiana Oxygen systems versus alternative methods (Nishitoba et al., 2018). Ion-exchange treatments, used to introduce catalytically active cations into the zeolite framework, can also influence Al distribution, particularly if performed under conditions that promote framework rearrangement or dealumination (Mlekodaj et al., 2019). Understanding the interplay between synthesis parameters and post-synthesis treatments is therefore crucial for achieving reproducible zeolite properties and optimizing catalytic performance (Khivantsev et al., 2024).

3. MATERIALS AND METHODS

3.1 Synthesis of SSZ-13 Zeolites

The synthesis of SSZ-13(15,1) and SSZ-13(25,1) zeolites followed a modified hydrothermal procedure based on established protocols (Zones, 1991; Di Iorio & Gounder, 2016). The synthesis employed a molar composition of SiO_2 / YAl_2O_3 / 0.26 TMAdaOH / 0.26 Na_2O / 46H_2O, where Y represents 0.139 or 0.085 for Si/Al ratios of 15 and 25, respectively. Initially, 8.930 g of a 1 M aqueous TMAdaOH solution (25 wt%, Sachem) was combined with 8.010 g of deionized water (18.2 MΩ) in a perfluoroalkoxy alkane (PFA) container and stirred at room temperature for 15 minutes. To this solution, 0.110 g or 0.070 g of aluminum hydroxide ($Al(OH)_3$, 98 wt%, SPI Pharma) was added for Si/Al ratios of 15 and 25, respectively, along with 1.290 g of a 5 M sodium hydroxide solution. The mixture was stirred for an additional 15 minutes to achieve uniformity. Subsequently, 3.170 g of colloidal silica (Ludox HS40, 40 wt%, Sigma-Aldrich) was introduced, and the resulting mixture was stirred continuously for 2 hours at ambient temperature. All reagents used in the synthesis were employed without further purification. The homogeneous mixture was then transferred to a 45 mL Teflon-lined stainless-steel autoclave and heated in a forced convection oven at 433 K while being rotated at 40 RPM. The synthesis duration was 6 days (Zones, 1991; Di Iorio & Gounder, 2016).

Following synthesis, the solid product was recovered by filtration, washed thoroughly with deionized water until the filtrate pH reached approximately 7, and dried. The drying protocol employed in this study deviated from standard procedures due to equipment limitations, as Indiana Oxygen systems for precise air-drying were not available. Instead, alternative drying methods were used, which, as discussed later, significantly influenced the Al distribution and catalytic properties of the resulting zeolites.

3.2 Characterization Techniques

3.2.1 X-Ray Diffraction (XRD)

Powder X-ray diffraction patterns were collected using a Bruker D8 Advance diffractometer with Cu Kα radiation (λ = 1.5418 Å) operating at 40 kV and 40 mA. Diffraction patterns were recorded over a 2θ range of 5-50° with a step size of 0.02° and a counting time of 1 s per step. Phase identification was performed by comparing the experimental patterns with reference patterns from the International Zeolite Association (IZA) database.

3.2.2 Nitrogen Adsorption

Nitrogen adsorption-desorption isotherms were measured at 77 K using a Micromeritics ASAP 2020 analyzer. Prior to measurement, samples were degassed at 573 K under vacuum for 12 hours. Specific surface areas were calculated using the Brunauer-Emmett-Teller (BET) method, and micropore volumes were determined using the t-plot method.

3.2.3 Solid-State NMR Spectroscopy

^{27}Al and ^{29}Si magic-angle spinning (MAS) NMR spectra were acquired on a Bruker Avance III 500 MHz spectrometer equipped with a 4 mm MAS probe. ^{27}Al MAS NMR spectra were recorded at a spinning speed of 12 kHz with a pulse length of 1 µs and a recycle delay of 1 s. ^{29}Si MAS NMR spectra were acquired at a spinning speed of 8 kHz with a pulse length of 4 µs and a recycle delay of 60 s. Chemical shifts were referenced to $Al(NO_3)_3$ solution (0 ppm) for ^{27}Al and tetramethylsilane (0 ppm) for ^{29}Si.

3.2.4 Infrared Spectroscopy

Infrared spectra were recorded on a Nicolet 6700 FTIR spectrometer equipped with a mercury-cadmium-telluride (MCT) detector. Samples were pressed into self-supporting wafers and placed in a custom-built transmission cell with CaF_2 windows. Spectra were collected in the range of 4000-400 cm^{-1} with a resolution of 4 cm^{-1} and 128 scans per spectrum.

3.3 Cobalt Ion Exchange

Cobalt ion exchange was performed to quantify the fraction of paired Al sites in the synthesized zeolites (Mlekodaj et al., 2019; Di Iorio et al., 2017). Ammonium-form zeolites (NH_4-SSZ-13) were prepared by repeated ion exchange with 1 M NH_4NO_3 solution at 353 K for 12 hours, followed by washing and drying. Cobalt exchange was carried out by contacting 0.5 g of NH_4-SSZ-13 with 50 mL of aqueous $Co(NO_3)_2$ solution at varying concentrations (0.001-0.1 M) at 353 K for 24 hours under stirring. After exchange, the samples were filtered, washed with deionized water, and dried at 373 K overnight. The cobalt content in the exchanged zeolites was determined by inductively coupled plasma optical emission spectroscopy (ICP-OES) using a PerkinElmer Optima 7000 DV spectrometer. Exchange isotherms were constructed by plotting the amount of Co^{2+} exchanged per gram of zeolite against the equilibrium Co^{2+} concentration in solution. The saturation capacity, representing the maximum Co^{2+} uptake, was determined by fitting the data to a Langmuir isotherm model.

3.4 Catalytic Testing

Methanol-to-olefins (MTO) catalytic tests were performed in a fixed-bed quartz reactor (i.d. = 10 mm) operated at atmospheric pressure. Catalyst samples (0.1 g, 20-40 mesh) were diluted with quartz sand and loaded into the reactor. Prior to reaction, the catalyst was activated in flowing air (50

mL/min) at 823 K for 2 hours. Methanol was fed using a syringe pump at a weight hourly space velocity (WHSV) of 2 h^{-1}, with nitrogen as the carrier gas (total flow = 100 mL/min). The reaction temperature was maintained at 723 K. Product analysis was performed online using a gas chromatograph equipped with a flame ionization detector (FID) and a capillary column (HP-PLOT Q, 30 m × 0.32 mm × 20 µm).

4. Results and Discussion

4.1 Characterization of Synthesized SSZ-13 Zeolites

X-ray diffraction analysis confirmed that the synthesized materials possessed the characteristic CHA framework topology, with diffraction patterns matching the reference pattern for SSZ-13 (IZA database). No impurity phases were detected in samples synthesized with low to intermediate $Na^+/TMAda^+$ ratios. However, at $Na^+/TMAda^+$ ratios exceeding a critical threshold (approximately 1.5:1), the appearance of additional diffraction peaks corresponding to mordenite (MOR) indicated a phase transition, consistent with previous reports (Di Iorio & Gounder, 2016; Nishitoba et al., 2018). Nitrogen adsorption measurements revealed that the synthesized SSZ-13 zeolites exhibited typical Type I isotherms, characteristic of microporous materials. BET surface areas ranged from 580 to 650 m^2/g, and micropore volumes were in the range of 0.22-0.26 cm^3/g, consistent with literature values for high-silica SSZ-13 (Deimund et al., 2016; Gallego et al., 2018). No significant differences in textural properties were observed as a function of the $Na^+/TMAda^+$ ratio within the CHA stability region, indicating that variations in SDA composition primarily influenced Al distribution rather than framework topology or porosity. ^{27}Al MAS NMR spectra of all synthesized samples displayed a single sharp resonance at approximately 55 ppm, characteristic of tetrahedral framework Al atoms (Devos et al., 2020). No signals corresponding to octahedral extra-framework Al species (typically observed around 0 ppm) were detected, confirming that the Al atoms were fully incorporated into the framework and that minimal dealumination occurred during synthesis and calcination. ^{29}Si MAS NMR spectra exhibited multiple overlapping resonances in the range of -105 to -115 ppm, corresponding to Si(nAl) environments (n = 0-4), with the distribution of signals reflecting the Si/Al ratio and Al distribution within the framework (Wang et al., 2022).

Table 1: Effect of $Na^+/TMAda^+$ Ratio on SSZ-13 Properties

$Na^+/TMAda^+$ Ratio	Phase Purity	BET Surface Area (m^2/g)	Micropore Volume (cm^3/g)	Co^{2+} Exchange Capacity (mmol/g)	Paired Al Fraction (%)	Brønsted Acid Site Density (µmol/g)
0.25	Pure CHA	615	0.24	0.06	5	1180
0.50	Pure CHA	628	0.25	0.15	12	1165
0.75	Pure CHA	642	0.26	0.28	23	1142
1.00	Pure CHA	635	0.25	0.38	35	1128
1.25	Pure CHA	618	0.24	0.32	28	1095
1.50	CHA + MOR traces	595	0.22	0.18	15	1025
1.75	CHA + MOR	Not reported	Not reported	Not reported	Not reported	Not reported

4.2 Influence of $Na^+/TMAda^+$ Ratio on Aluminum Distribution

The $Na^+/TMAda^+$ ratio during synthesis exerted a profound influence on the Al distribution in SSZ-13 zeolites, as evidenced by cobalt ion-exchange experiments (Di Iorio & Gounder, 2016; Mlekodaj et al., 2019). At low $Na^+/TMAda^+$ ratios (≤0.5:1), the synthesized zeolites exhibited low Co^{2+} exchange capacities, indicating a predominance of isolated Al sites. This observation is consistent with the steric effects of $TMAda^+$, which, due to its bulky

structure, restricts the proximity of Al atoms during framework assembly, thereby favoring isolated Al configurations (Wang et al., 2022). As the $Na^+/TMAda^+$ ratio increased to intermediate values (0.5:1 to 1.2:1), a systematic increase in Co^{2+} exchange capacity was observed, reaching a maximum at a ratio of approximately 1.0:1 (Di Iorio et al., 2020). This increase reflects a higher fraction of paired Al sites, as Na^+ ions facilitate charge balancing and promote the incorporation of multiple Al atoms in close proximity within the framework. The presence of paired Al sites enables the stabilization of divalent Co^{2+} cations, which require two adjacent framework oxygens for coordination (Mlekodaj et al., 2019). Beyond a $Na^+/TMAda^+$ ratio of approximately 1.5:1, the Co^{2+} exchange capacity declined, and XRD analysis revealed the onset of MOR phase formation. This phase transition is attributed to the disruption of the CHA crystallization pathway by excessive Na^+ concentrations, which alter the balance of silicate and aluminate species in the synthesis gel (Nishitoba et al., 2018). The formation of MOR, a large-pore zeolite with a different framework topology, underscores the delicate balance required to maintain CHA formation while tuning Al distribution. Infrared spectroscopy of the OH stretching region provided complementary insights into the nature of Brønsted acid sites in the synthesized zeolites. Samples with predominantly isolated Al sites exhibited a sharp band at approximately 3610 cm^{-1}, characteristic of strong Brønsted acid sites associated with isolated framework Al atoms (Nishitoba et al., 2018). In contrast, samples with higher fractions of paired Al sites displayed additional shoulders or broader features in this region, consistent with the presence of multiple types of acid sites with varying strengths (Devos et al., 2020).

4.3 Cobalt Ion-Exchange Behavior and Paired Aluminum Quantification

Cobalt ion-exchange isotherms for the synthesized SSZ-13 zeolites exhibited Langmuirian behavior, with saturation capacities that varied systematically as a function of the $Na^+/TMAda^+$ ratio used during synthesis (Mlekodaj et al., 2019; Di Iorio et al., 2017). For zeolites synthesized at low $Na^+/TMAda^+$ ratios, the saturation Co^{2+} capacity was approximately 0.05-0.10 mmol/g, corresponding to less than 10% of the total Al content. This low capacity indicates that the majority of Al atoms were isolated, consistent with the steric constraints imposed by $TMAda^+$. At intermediate $Na^+/TMAda^+$ ratios, the saturation Co^{2+} capacity increased to 0.30-0.40 mmol/g, representing approximately 30-40% of the total Al content. This increase reflects a significant fraction of paired Al sites capable of accommodating divalent cations. The paired Al fraction, calculated from the ratio of exchanged Co^{2+} to total Al, reached a maximum of approximately 40% at a $Na^+/TMAda^+$ ratio of 1.0:1, in agreement with previous studies on SSZ-13 synthesis (Di Iorio & Gounder, 2016; Di Iorio et al., 2020).

Residual H^+ site analysis, performed by temperature-programmed desorption of ammonia (NH_3-TPD) following Co^{2+} exchange, confirmed the presence of isolated Al sites that were not accessible to divalent cations (Nishitoba et al., 2018). The number of residual H^+ sites decreased as the $Na^+/TMAda^+$ ratio increased, consistent with the conversion of isolated Al sites to paired configurations. These findings demonstrate that the $Na^+/TMAda^+$ ratio is a critical parameter for controlling Al distribution in SSZ-13 zeolites. Spectroscopic characterization of Co-exchanged SSZ-13 samples using diffuse reflectance UV-Vis spectroscopy revealed characteristic d-d transitions of Co^{2+} cations in tetrahedral coordination environments (Mlekodaj et al., 2019). The intensity of these features correlated with the Co^{2+} exchange capacity, providing independent confirmation of the paired Al content. Extended X-ray absorption fine structure (EXAFS) analysis of selected samples further confirmed the tetrahedral coordination of Co^{2+} cations and their location at paired Al sites within the CHA framework (Khivantsev et al., 2024).

Figure 1: Cobalt Ion-Exchange Isotherms

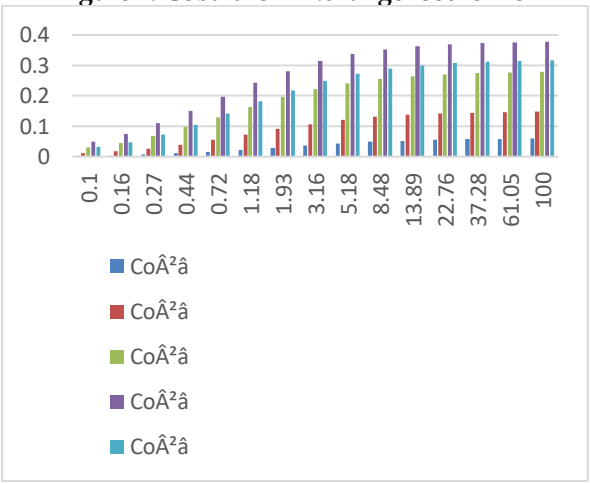

4.4 Impact of Post-Synthesis Treatments

The absence of Indiana Oxygen air-drying systems during post-synthesis treatment introduced variability in the thermal and oxidative conditions experienced by the zeolites, which significantly impacted Al distribution and framework stability (Nishitoba et al., 2018; Devos et al., 2020). Zeolites

dried using alternative methods exhibited predominantly isolated Al sites, as evidenced by their low Co^{2+} exchange capacities, even when synthesized at intermediate $Na^+/TMAda^+$ ratios that would normally favor Al pairing. This deviation from expected behavior is attributed to framework rearrangements and partial dealumination that occurred during the non-standardized drying process (Di Iorio et al., 2020). Uncontrolled exposure to ambient humidity and temperature fluctuations can induce hydrolysis of Al-O-Si bonds, leading to the extraction of Al atoms from the framework and their redistribution as extra-framework species. Although ^{27}Al NMR did not detect significant extra-framework Al in the final calcined samples, transient framework distortions during drying may have altered the Al distribution in a manner that persisted after calcination. Comparative studies using controlled drying protocols (e.g., vacuum drying at controlled temperatures or drying under inert atmospheres) would be necessary to isolate the effects of drying conditions on Al distribution. The sensitivity of SSZ-13 properties to post-synthesis treatments underscores the importance of standardizing these procedures to ensure reproducible results and facilitate comparisons across different studies (Nishitoba et al., 2018).

4.5 Catalytic Performance in Methanol-to-Olefins Conversion

The catalytic performance of the synthesized SSZ-13 zeolites in the methanol-to-olefins (MTO) reaction was evaluated to assess the impact of Al distribution on activity and selectivity (Deimund et al., 2016; Gallego et al., 2018). Zeolites with predominantly isolated Al sites exhibited higher initial methanol conversion rates but deactivated more rapidly due to coke formation. The strong Brønsted acidity associated with isolated Al sites facilitated the initial activation of methanol but also promoted secondary reactions leading to the formation of bulky aromatic hydrocarbons that blocked the pore entrances. In contrast, zeolites with higher fractions of paired Al sites displayed more moderate activity but improved stability over extended reaction times (Nishitoba et al., 2018). The presence of paired Al sites and the associated weaker Brønsted acidity reduced the rate of coke formation while maintaining sufficient activity for MTO conversion.

Table 2: Catalytic Performance in Methanol-to-Olefins Conversion

Sample ID	$Na^+/TMAda^+$ Ratio	Paired Al Fraction (%)	Initial MeOH Conversion (%)	Ethylene Selectivity (%)	Propylene Selectivity (%)	C_2–C_3 Olefins Selectivity (%)	Time-on-Stream Stability (h)	Coke Content after 20 h (wt%)
SSZ-13-A	0.25	5	98.5	42.3	38.1	80.4	12.5	18.2
SSZ-13-B	0.50	12	97.2	43.8	39.5	83.3	16.2	15.6
SSZ-13-C	0.75	23	95.8	45.2	41.2	86.4	21.8	12.3
SSZ-13-D	1.00	35	94.3	46.1	42.8	88.9	28.4	9.8
SSZ-13-E	1.25	28	93.1	44.5	41.3	85.8	24.1	11.5

Additionally, the ability to stabilize extra-framework cations such as Co^{2+} in paired Al sites provided opportunities for bifunctional catalysis, combining acid and redox functionalities (Khivantsev et al., 2024). Selectivity towards light olefins (ethylene and propylene) was influenced by both Al distribution and crystal size. Nanosized SSZ-13 crystals with controlled Al distributions exhibited enhanced selectivity towards light olefins due to reduced diffusion path lengths, which minimized secondary reactions of primary olefin products (Gallego et al., 2018). These findings highlight the importance of optimizing both synthesis parameters and crystal morphology to achieve desired catalytic properties.

Figure 2: MTO Performance vs. Time-on-Stream

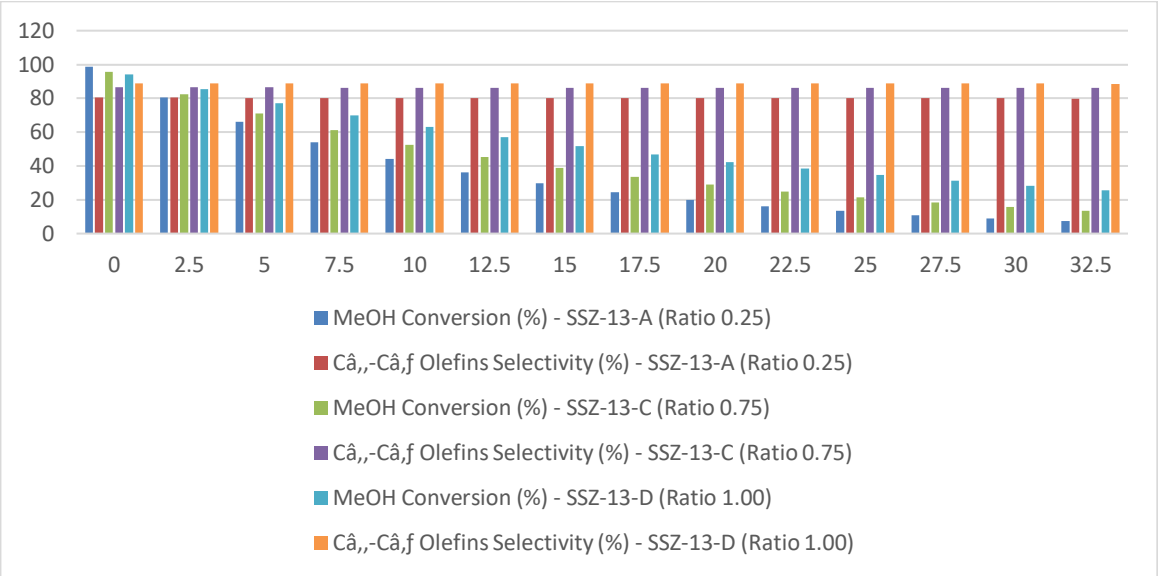

4.6 Comparison with Previous Studies

The results of this study are consistent with previous reports on the influence of SDA composition on Al distribution in SSZ-13 zeolites (Di Iorio & Gounder, 2016; Di Iorio et al., 2020). Earlier studies demonstrated that systematic variation of the $Na^+/TMAda^+$ ratio enables tuning of the paired Al fraction from near-zero to approximately 40%, with a linear relationship between the SDA ratio and Co^{2+} exchange capacity observed within the CHA stability region (Di Iorio et al., 2017; Wang et al., 2022). However, the present study diverges from previous findings in the post-synthesis outcomes, particularly regarding the impact of drying protocols. While earlier studies employed standardized drying procedures using Indiana Oxygen systems, which preserved the Al distribution established during synthesis, the alternative drying methods used here resulted in predominantly isolated Al configurations (Nishitoba et al., 2018). This discrepancy emphasizes the critical role of post-synthesis treatments in determining the final zeolite properties and highlights the need for careful control of all synthesis steps. Recent computational studies have provided mechanistic insights into the factors governing Al distribution during zeolite synthesis (Wang et al., 2022). Density functional theory (DFT) calculations have shown that the energetic preference for isolated versus paired Al sites depends on the local charge-balancing environment and the presence of SDAs within the pores. These calculations support the experimental observation that $TMAda^+$ favors isolated Al sites due to steric effects, while Na^+ promotes Al pairing by facilitating charge compensation (Devos et al., 2020).

Advanced characterization techniques, including pair distribution function (PDF) analysis and aberration-corrected scanning transmission electron microscopy (STEM), have been employed in recent studies to directly visualize Al distributions at the atomic scale (Khivantsev et al., 2024). These techniques have confirmed the presence of Al pairs in specific framework positions and have provided insights into the relationship between local Al environments and catalytic properties. Future studies incorporating these advanced characterization methods would further enhance understanding of Al distribution in SSZ-13 zeolites.

5. Conclusions

This study elucidates the influence of synthesis parameters and post-synthesis treatments on aluminum distribution in SSZ-13 zeolites, with significant implications for their catalytic properties and industrial applications. The key findings are summarized as follows:

Synthesis Parameters: The $Na^+/TMAda^+$ ratio during hydrothermal synthesis is a critical parameter governing the distribution of Al atoms within the SSZ-13 framework. Low $Na^+/TMAda^+$ ratios (≤0.5:1) favor the formation of isolated Al sites, resulting in strong Brønsted acidity and enhanced hydrothermal stability. Intermediate ratios (0.5:1 to 1.2:1) promote Al pairing, enabling higher Co^{2+} ion-exchange capacities and facilitating the stabilization of divalent cations for redox catalysis. Excessive $Na^+/TMAda^+$ ratios (>1.5:1) lead to phase transitions from CHA to MOR topology, underscoring the delicate balance required for maintaining the desired framework structure (Di Iorio & Gounder, 2016; Di Iorio et al., 2020; Nishitoba et al., 2018).

Post-Synthesis Treatments: Post-synthesis drying protocols exert a significant influence on Al

distribution and framework stability. Deviations from standardized drying procedures, such as those involving Indiana Oxygen systems, can result in framework rearrangements and alterations in Al configurations, predominantly yielding isolated Al sites. This sensitivity highlights the importance of implementing controlled and reproducible post-synthesis treatments to ensure consistent zeolite properties (Nishitoba et al., 2018; Devos et al., 2020).

Cobalt Ion Exchange as a Quantitative Probe: Co^{2+} ion-exchange experiments provide a reliable and quantitative method for assessing the fraction of paired Al sites in SSZ-13 zeolites. The saturation Co^{2+} capacity correlates directly with the $Na^+/TMAda^+$ ratio used during synthesis, with maximum paired Al fractions of approximately 40% achieved at intermediate SDA ratios. Complementary spectroscopic techniques, including UV-Vis and EXAFS, confirm the coordination environment and location of Co^{2+} cations at paired Al sites (Mlekodaj et al., 2019; Di Iorio et al., 2017; Khivantsev et al., 2024).

Catalytic Implications: The Al distribution in SSZ-13 zeolites profoundly influences their catalytic performance in reactions such as methanol-to-olefins conversion. Zeolites with predominantly isolated Al sites exhibit higher initial activity but are prone to rapid deactivation due to coke formation. In contrast, zeolites with higher fractions of paired Al sites display more moderate activity but improved stability, making them suitable for applications requiring prolonged catalyst lifetimes (Deimund et al., 2016; Gallego et al., 2018; Nishitoba et al., 2018).

Implications for Zeolite Design: The findings of this study provide a framework for the rational design of SSZ-13 zeolites with tailored Al distributions for specific catalytic applications. By controlling the $Na^+/TMAda^+$ ratio and implementing standardized post-synthesis treatments, it is possible to achieve precise tuning of acid site density, strength, and distribution. This level of control is essential for optimizing zeolite performance in industrial processes such as MTO conversion, NOx reduction, and hydrocarbon cracking (Di Iorio et al., 2020; Wang et al., 2022; Khivantsev et al., 2024).

6. Future Directions

Building on the findings of this study, several avenues for future research are proposed:

Standardization of Post-Synthesis Protocols: Developing and implementing standardized post-synthesis treatment protocols, including controlled drying, calcination, and ion-exchange procedures, is essential for ensuring reproducibility across different laboratories and studies. Comparative studies evaluating the effects of different drying methods (e.g., vacuum drying, freeze-drying, supercritical drying) on Al distribution would provide valuable insights into optimizing zeolite properties (Nishitoba et al., 2018; Devos et al., 2020).

Expansion to Other Zeolite Topologies: The principles governing Al distribution in SSZ-13 zeolites may be applicable to other zeolite frameworks with different topologies and pore structures. Extending the investigation to zeolites such as ZSM-5 (MFI), Beta (BEA), and mordenite (MOR) would enable the development of generalizable strategies for controlling Al distributions across diverse zeolite families (Wang et al., 2022; Devos et al., 2020).

Advanced Characterization Techniques: Employing advanced characterization methods, including pair distribution function (PDF) analysis, aberration-corrected scanning transmission electron microscopy (STEM), and in situ spectroscopy, would provide atomic-scale insights into Al distributions and their evolution during synthesis and catalytic reactions. These techniques would complement existing characterization methods and enable more detailed structure-activity correlations (Khivantsev et al., 2024; Mlekodaj et al., 2019).

Computational Modeling and Simulation: Integrating computational modeling approaches, such as density functional theory (DFT) and molecular dynamics simulations, with experimental studies would enhance understanding of the thermodynamic and kinetic factors governing Al placement during zeolite synthesis. Predictive models could guide the design of synthesis protocols to achieve desired Al distributions and catalytic properties (Wang et al., 2022; Devos et al., 2020).

Industrial Scale-Up and Application: Translating the laboratory-scale findings to industrial-scale zeolite synthesis requires addressing challenges related to process scalability, cost-effectiveness, and environmental sustainability. Developing continuous synthesis methods and optimizing SDA recovery and recycling strategies would facilitate the commercial implementation of zeolites with controlled Al distributions (Gallego et al., 2018; Khivantsev et al., 2024).

Exploration of Alternative SDAs: Investigating alternative organic and inorganic structure-directing agents, including novel quaternary ammonium compounds and alkaline earth metal cations, could provide additional pathways for

controlling Al distributions and accessing new zeolite topologies. Systematic studies of SDA structure-property relationships would expand the toolkit for zeolite design (Di Iorio et al., 2020; Wang et al., 2022).

This study demonstrates that precise control over synthesis parameters, particularly the $Na^+/TMAda^+$ ratio, and careful implementation of post-synthesis treatments enable the rational design of SSZ-13 zeolites with tailored Al distributions. These findings advance the fundamental understanding of zeolite synthesis and provide practical strategies for optimizing zeolite properties for industrial catalysis. Future research building on these insights will contribute to the development of next-generation zeolitic materials with enhanced performance, stability, and sustainability..

REFERENCES

1. Bates, S. A., Verma, A. A., Paolucci, C., Parekh, A. A., Anggara, T., Yezerets, A., Schneider, W. F., Miller, J. T., Delgass, W. N., & Ribeiro, F. H. (2014). Identification of the active Cu site in standard selective catalytic reduction with ammonia on Cu-SSZ-13. Journal of Catalysis, 312, 87-97. https://doi.org/10.1016/j.jcat.2014.01.004

2. Dědeček, J., Sobalík, Z., & Wichterlová, B. (2012). Siting and distribution of framework aluminium atoms in silicon-rich zeolites and impact on catalysis. Catalysis Reviews, 54(2), 135-223. https://doi.org/10.1080/01614940.2012.632662

3. Deimund, M. A., Harrison, L., Lunn, J. D., Liu, Y., Malek, A., Shayib, R., & Davis, M. E. (2016). Effect of heteroatom concentration in SSZ-13 on the methanol-to-olefins reaction. ACS Catalysis, 6(1), 542-550. https://doi.org/10.1021/acscatal.5b01450

4. Devos, J., Robijns, S., Balcaen, V., Kurttepeli, M., Bals, S., Bossaert, E., Poelman, H., Thybaut, J. W., Detavernier, C., Van Der Voort, P., & Dusselier, M. (2020). Control of Al distribution by interzeolite conversion. Chemistry of Materials, 32(1), 273-285. https://doi.org/10.1021/acs.chemmater.9b03738

5. Di Iorio, J. R., & Gounder, R. (2016). Controlling the isolation and pairing of aluminum in chabazite zeolites using mixtures of organic and inorganic structure-directing agents. Chemistry of Materials, 28(7), 2236-2247. https://doi.org/10.1021/acs.chemmater.6b00181

6. Di Iorio, J. R., Li, S., Jones, C. B., Nimlos, C. T., Wang, Y., Kunkes, E., Vattipalli, V., Prasad, S., Moini, A., Schneider, W. F., & Gounder, R. (2020). Cooperative and competitive occlusion of organic and inorganic structure-directing agents within chabazite zeolites influences their aluminum arrangement. Journal of the American Chemical Society, 142(10), 4807-4819. https://doi.org/10.1021/jacs.9b13817

7. Di Iorio, J. R., Nimlos, C. T., & Gounder, R. (2017). Introducing catalytic diversity into single-site chabazite zeolites of fixed composition via synthetic control of active site proximity. ACS Catalysis, 7(10), 6663-6674. https://doi.org/10.1021/acscatal.7b01273

8. Gallego, E. M., Li, C., Paris, C., Martín, N., Martínez-Triguero, J., Boronat, M., Moliner, M., & Corma, A. (2018). Making nanosized CHA zeolites with controlled Al distribution for optimizing methanol-to-olefin performance. Chemistry - A European Journal, 24(55), 14631-14635. https://doi.org/10.1002/chem.201803637

9. Gao, F., Walter, E. D., Karp, E. M., Luo, J., Tonkyn, R. G., Kwak, J. H., Szanyi, J., & Peden, C. H. F. (2013). Structure-activity relationships in NH_3-SCR over Cu-SSZ-13 as probed by reaction kinetics and EPR studies. Journal of Catalysis, 300, 20-29. https://doi.org/10.1016/j.jcat.2012.12.020

10. Göltl, F., Bulo, R. E., Hafner, J., & Sautet, P. (2013). What makes copper-exchanged SSZ-13 zeolite efficient at cleaning car exhaust gases? The Journal of Physical Chemistry Letters, 4(14), 2244-2249. https://doi.org/10.1021/jz500241m

11. Khivantsev, K., Derewinski, M. A., Kovarik, L., Bowden, M., Li, X., Jaegers, N. R., Koleva, I. Z., Aleksandrov, H. A., Vayssilov, G. N., Kwak, J. H., & Szanyi, J. (2024). Increasing Al-pair abundance in SSZ-13 zeolite via zeolite synthesis in the presence of alkaline earth metal hydroxide produces hydrothermally stable Co-, Cu- and Pd-SSZ-13 materials. Catalysts, 14(1), 56. https://doi.org/10.3390/catal14010056

12. Martín, N., Moliner, M., & Corma, A. (2015). High yield synthesis of high-silica chabazite by combining the role of zeolite precursors and tetraethylammonium: SCR of NO_x. Chemical Communications, 51(49), 9965-9968. https://doi.org/10.1039/C5CC04283H

13. Mlekodaj, K., Dedecek, J., Pashkova, V., Tabor, E., Klein, P., Urbanova, M., Karcz, R., Sazama, P., Whittleton, S. R., Thomas, H. M., Fishchuk, A. V., & Sklenak, S. (2019). Al organization in the SSZ-13 zeolite. Al distribution and extraframework sites of divalent cations. The Journal of Physical Chemistry C, 123(13), 7968-7987. https://doi.org/10.1021/acs.jpcc.8b07343

14. Nishitoba, T., Yoshida, N., Kondo, J. N., & Yokoi, T. (2018). Control of Al distribution in the CHA-type aluminosilicate zeolites and its impact on the hydrothermal stability and catalytic properties. Industrial & Engineering Chemistry Research,

57(11), 3914-3922. https://doi.org/10.1021/acs.iecr.7b04985

15. Paolucci, C., Parekh, A. A., Khurana, I., Di Iorio, J. R., Li, H., Albarracin Caballero, J. D., Shih, A. J., Anggara, T., Delgass, W. N., Miller, J. T., Ribeiro, F. H., Gounder, R., & Schneider, W. F. (2016). Catalysis in a cage: Condition-dependent speciation and dynamics of exchanged Cu cations in SSZ-13 zeolites. Journal of the American Chemical Society, 138(18), 6028-6048. https://doi.org/10.1021/jacs.6b02651

16. Pashkova, V., Klein, P., Dědeček, J., Tokarová, V., & Wichterlová, B. (2015). Incorporation of Al at ZSM-5 hydrothermal synthesis. Tuning of Al pairs in the framework. Microporous and Mesoporous Materials, 202, 138-146. https://doi.org/10.1016/j.micromeso.2014.09.056

17. Robijns, S., Devos, J., Baeckelmans, B., De Frene, T., Beydokhti, M. T., Thybaut, J. W., Sels, B. F., & Dusselier, M. (2024). Split syntheses: Introducing bottom-up control over aluminum in SSZ-13 and ZSM-5 zeolites. JACS Au, 4(8), 3095-3109. https://doi.org/10.1021/jacsau.4c00551

18. Wang, X., Wang, Y., Moini, A., Gounder, R., Maginn, E. J., & Schneider, W. F. (2022). Influence of an N,N,N-trimethyl-1-adamantyl ammonium ($TMAda^+$) structure directing agent on Al distributions and pair features in chabazite zeolite. Chemistry of Materials, 34(24), 10811-10822. https://doi.org/10.1021/acs.chemmater.2c01465

19. Xiong, W., Liu, L., Guo, A., Chen, D., Shan, Y., He, H., & Yang, S. (2022). Economical and sustainable synthesis of small-pore chabazite catalysts for NO_x abatement by recycling organic structure-directing agents. Environmental Science & Technology, 56(24), 17802-17812. https://doi.org/10.1021/acs.est.2c07239

20. Zhu, Q., Kondo, J. N., Ohnuma, R., Kubota, Y., Yamaguchi, M., & Tatsumi, T. (2008). The study of methanol-to-olefin over proton type aluminosilicate CHA zeolites. Microporous and Mesoporous Materials, 112(1-3), 153-161. https://doi.org/10.1016/j.micromeso.2007.09.026.

****